

Influence of oxygen stoichiometry on the irreversible magnetization and flux creep in $R\text{Ba}_2\text{Cu}_3\text{O}_{7-\delta}$ ($R = \text{Y, Tm}$) single crystals

A. A. Zhukov

*Kernforschungszentrum Karlsruhe, Institut für Technische Physik, Postfach 3640, D-76021 Karlsruhe, Germany
and Physics Department, Moscow State University, Moscow 117234, Russia*

H. Küpfer

Kernforschungszentrum Karlsruhe, Institut für Technische Physik, Postfach 3640, D-76021 Karlsruhe, Germany

G. Perkins, L. F. Cohen, and A. D. Caplin

*Centre for High Temperature Superconductivity, Blackett Laboratory, Imperial College,
London SW72BZ, United Kingdom*

S. A. Klestov

Physics Department, Moscow State University, Moscow 117234, Russia

H. Claus

Kernforschungszentrum Karlsruhe, Institut für Technische Physik, Postfach 3640, D-76021 Karlsruhe, Germany

V. I. Voronkova

Physics Department, Moscow State University, Moscow 117234, Russia

T. Wolf and H. Wühl

Kernforschungszentrum Karlsruhe, Institut für Technische Physik, Postfach 3640, D-76021 Karlsruhe, Germany

(Received 14 December 1994)

The influence of the oxygen stoichiometry on magnetization and relaxation of $R\text{Ba}_2\text{Cu}_3\text{O}_{7-\delta}$ ($R = \text{Y, Tm}$) single crystals was studied for $0 \leq \delta \leq 0.55$. The field dependences of the shielding currents $j_s(H)$ and flux creep rates $S(H)$ were analyzed. Three different kinds of $j_s(H)$ and $S(H)$ behavior can be seen in highly oxygenated samples ($\delta < 0.1$). (i) At high temperatures, $j_s(H)$ shows a common fishtail peak, which is present for all oxygen contents. The field position and height of the j_s peak increase rapidly with decreasing δ . Approaching the stoichiometric state $\delta=0$, the value of the current starts to decrease with lower oxygen deficiency, in contrast to the still increasing irreversibility field B_{irr} . This points to the importance of oxygen disorder for the pinning and stresses the melting nature of the irreversibility line. The peak position B_{max} is found to correlate with B_{irr} . A possible relation of the fishtail with a synchronization effect and with the vanishing of C_{66} at the melting transition is proposed. (ii) In the intermediate-temperature region, some of the samples showed a new second peak with weak temperature and δ dependence. The probable origin of this feature is matching with twin structure. This peak disappears for $\delta > 0.1$, when the fishtail position shifts below the matching field. (iii) The low-temperature region is characterized by a monotonic decrease of $j_s(B)$. This region becomes narrower with larger δ and disappears for $\delta > 0.3$. Thus in highly deoxygenated samples, the fishtail feature is observed for practically all temperatures. The possible connection of the low-temperature region with the pinning of the small vortex bundles or with the slipping of vortices along the twin planes is considered.

INTRODUCTION

The maximum of the current vs magnetic field above the self-field region in high-temperature superconductors (HTSC) is often called the fishtail or butterfly effect.^{1,2} In contrast to the peak effect in conventional superconductors, the position of the maximum of the current in HTSC is significantly below the upper critical field $H_{c2}(T)$. Several mechanisms were proposed for the explanation of this feature in HTSC (Refs. 1–5) and in conventional superconductors.^{6–11} For the $R\text{Ba}_2\text{Cu}_3\text{O}_{7-\delta}$ system two possible explanations are widely discussed. In

the first, the increase of the current is associated with the presence of regions of oxygen-deficient or of another phase which become normal with increasing magnetic field.^{1–3,5} The second explanation⁴ is based on the collective creep mechanism and proposes that the unrelaxed critical current does not have the anomalous increase with magnetic field; the increase of the measured current is caused by the slower relaxation (steeper E - j curves) at higher magnetic field.

In this work we report the observation of a second peak¹² arising at intermediate temperatures in addition to the conventional fishtail peak: we also describe the

influence of oxygen content on the fishtail effect and this new feature. Different types of behavior for the magnetization and flux-creep rate are distinguished and analyzed. The changes in oxygen stoichiometry allow one to vary the intrinsic parameters and the properties of hypothetical second-phase or pinning centers. Consequently, the explanations proposed for the fishtail effect can be tested.

EXPERIMENT

Two sets of carefully prepared $R\text{Ba}_2\text{Cu}_3\text{O}_{7-\delta}$ ($R = \text{Y}, \text{Tm}$) single crystals were studied. Variations of oxygen stoichiometry were produced by long-time annealing (up to 500 h) at different temperatures with normal (1 bar) and high (200 bars) oxygen pressure. The oxygen content was determined from c -axis lattice parameter using the relation $\delta = 74.49 - 5.78c [\text{\AA}]$ (Ref. 13) and from a previous calibration of $T_c(\delta)$.^{14,15} The gradual variation of annealing temperature allowed discrimination between overdoped and underdoped states in each side of the $T_c(\delta)$ maximum. The superconducting transition temperature changed from 56.5 to 92.7 K and the width of the superconducting transition varied from less than 0.5 K for $\delta \leq 0.1$ up to 2 K for lower oxygen concentrations.

The studies were made on two different series of samples. In the first case a set of $\text{TmBa}_2\text{Cu}_3\text{O}_{7-\delta}$ single crystals (Z1–Z6) taken from the same batch¹⁶ were used. To test the uniformity of the studied samples, the values of the shielding current density in the initial state were compared for $T = 50$ K. They coincided within 10%, confirming the similarity of the $\text{TmBa}_2\text{Cu}_3\text{O}_{7-\delta}$ crystals that were used.

In the second series, two $\text{YBa}_2\text{Cu}_3\text{O}_{7-\delta}$ single crystals (WU3 and WU4) grown as described elsewhere¹⁷ were annealed at different temperatures. This provided the variation of oxygen stoichiometry in the same sample. The reversible character of this procedure was proven by the reproducibility of the measured parameters after repeated oxygenation. One of the $\text{YBa}_2\text{Cu}_3\text{O}_{7-\delta}$ crystals (WU2) was annealed at 200 bars oxygen at $T = 370^\circ\text{C}$ to obtain $\delta = (0 \pm 0.02)$, as proved by neutron diffraction. We shall also present data for a $\text{YBa}_2\text{Cu}_3\text{O}_{6.96}$ single crystal (TWH) with the pronounced double-peak structure. The parameters of the studied samples are given in Table I. These samples represent common behavior observed in our extensive studies of a large set of single crystals and melt-textured samples with different stoichiometry and microstructure.¹⁸

The shielding current density j_s was determined from magnetization measurements performed with a vibration sample magnetometer, for the magnetic field $H \leq 120$ kOe parallel to the c axis. The field was cycled with different constant sweep rates. The shielding current

densities were calculated from hysteresis width using the Bean relation for a disk, which has been shown¹⁹ to be a good approximation in the case of sharp E - j dependence. The j_s values were usually taken for the sweep rate of the magnetic field 120 Oe/s, which corresponds to the electric field $E \approx 10^{-7}$ V/cm. The relaxation rate was determined by applying regression analysis to 5–10 such loops, with sweep rates of the magnetic field $\dot{H} = dH/dt$ ranging typically from 3 to 12 mT/s.^{20,21} The absolute relaxation rate $R = dM/d \ln \dot{H}$ was calculated for both decreasing and increasing magnetic field. To exclude the reversible magnetization, the normalized relaxation rate S was usually determined from hysteresis width ΔM using relation $S = d \ln \Delta M / d \ln \dot{H}$. The superconducting transition temperature T_c was determined from onset of diamagnetic signal at $H = 5$ Oe.

RESULTS

Three different types of $m(H)$ behavior may be distinguished in the studied $R\text{Ba}_2\text{Cu}_3\text{O}_{7-\delta}$ single crystals. This is in accordance with previous observations.^{4,22} The characteristic feature of the first type is a sharp $m(H)$ peak well above self-field region. For the second case the increase of hysteresis width Δm is followed by the broad field region with nearly constant Δm . The third type corresponds to the conventional monotonic decrease of $m(H)$ with magnetic field. Three different kinds of $m(H)$ behavior are associated with sharp distinctions in the flux creep and the influence of oxygen stoichiometry. Further we shall give a detailed description for each of these types separately.

The well-pronounced $m(H)$ peak is observed in the high-temperature region just below T_c . It is characterized by the peak position which shifts to higher fields with decreasing temperature. Following Refs. 1–3 and 5, we shall refer to this temperature interval as the region of conventional fishtail behavior. The decrease of oxygen content broadens this interval but does not suppress the fishtail feature. In Fig. 1, it is shown the magnetization hysteresis curves for the fully oxygenated sample $y = (7.00 \pm 0.02)$, and for the single crystal with large oxygen deficiency $y = (6.48 \pm 0.05)$. For all studied samples, independently of the oxygen content the fishtail appears (1–4) K below T_c , and shows a similar $j(H)$ shape and a ratio $H_{\text{irr}}/H_{\text{max}} = 2$ –4. The disappearance of the peak near T_c is observed roughly in the region of the superconducting transition and probably originates from the inhomogeneity-induced smearing. The ratio $H_{\text{irr}}/H_{\text{max}}$ usually increases in samples having broader transition. Lower oxygen causes only a decrease of H_{max} and j_{max} values.

As was mentioned before, the behavior of H_{max} corre-

TABLE I. Parameters of the studied $R\text{Ba}_2\text{Cu}_3\text{O}_{7-\delta}$ single crystals.

Sample	Z5	Z4	Z2	Z1	Z6	Z3	WU2	WU3	WU4	TWH
R	Tm	Tm	Tm	Tm	Tm	Tm	Y	Y	Y	Y
$7-\delta$	6.45	6.48	6.62	6.68	6.69	6.90	7.00	6.94	6.96	6.94
T_c (K)	56.5	57.8	68.5	82.0	84.5	91.0	88.8	92.7	90.7	92.5

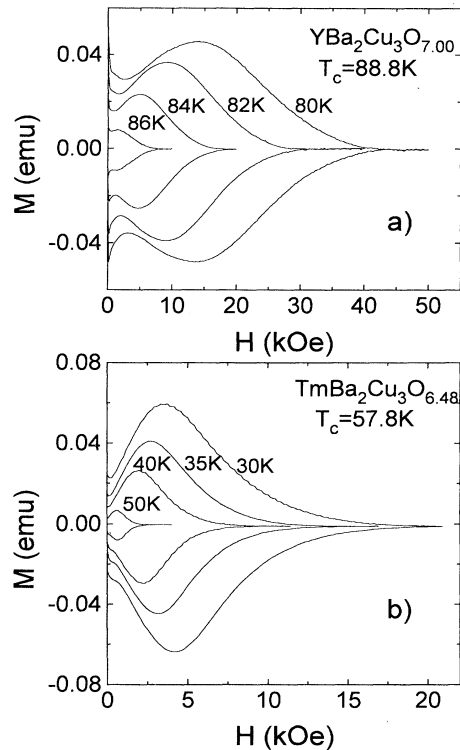


FIG. 1. The magnetic-field dependences of the magnetization in the region of conventional fishtail behavior for (a) fully oxidized $\text{YBa}_2\text{Cu}_3\text{O}_y$ (WU2, $y=7.00\pm 0.02$) and (b) high oxygen-deficient $\text{TmBa}_2\text{Cu}_3\text{O}_y$ (Z4, $y=6.48\pm 0.05$) single crystals.

lates with H_{irr} . Such correlation provides scaling of the $j(H)$ dependence already discussed in Refs. 3, 5, 22, and 23. The proposed scaling laws differ in the values used for scaling field and current; however, they are all equivalent in the case of the universal $j_s(H)$ behavior observed. Following Ref. 3 we use the peak position $H_{\text{max}}(T)$ for the characteristic scaling parameters in the universal scaling relation $j_s(H, T)/j_s(H_{\text{max}}, T) = f[H/H_{\text{max}}(T)]$ with a temperature-independent function f . The quality of the scaling is somewhat sample-dependent (Fig. 2) which is probably connected with sample inhomogeneity and twin structure. For the samples studied the scaling breaks down at intermediate temperatures [Fig. 2(a)]. However, the untwinned $\text{TmBa}_2\text{Cu}_3\text{O}_{7-\delta}$ single crystal³ kept scaling behavior down to the low-temperature region. To stress the importance of scaling, it is worth mentioning that the variations of H_{max} and $j(H_{\text{max}})$ in the interval 72–88 K [Fig. 2(a)] exceed one order in magnitude.

With the increase of oxygen content, the maximum value of the current and its field position at first monotonically increase. However, such behavior changes approaching the fully oxygenated state. As can be seen from Figs. 3(a) and 3(b), at high temperatures the values of the current j_s start to decrease, whereas H_{max} and H_{irr} continue to grow with decreasing δ . This is in accordance with the results of Ref. 1. For higher temperatures the decrease of j_s is observed for larger δ values [Fig.

3(a)]. These large changes in j_s cannot be connected with variations of T_c which is nearly the same in states 1–3 (1–92.1 K, 2–92.7 K, 3–92.3 K) and decreases significantly only for the most deoxygenated states (4–88.5 K, 5–82.9 K). In contrast to the high-temperature behavior, the shielding current at low T increases monotonically with oxygen concentration [Fig. 3(c)]. It is worth mentioning that we have observed an enhancement of the irreversibility line up to 10 T at 77 K, which is above any value reported before. However this large increase of H_{irr} is always associated with a reduced current.

The normalized relaxation rates in the region of the fishtail feature for all studied samples have a characteristic universal behavior^{21,24} presented in Figs. 4(a) and 4(b) for fully and highly deoxygenated samples, respectively. Initially, $S(H)$ decreases with magnetic field, and has a minimum at the field corresponding approximately to the one-half of the position of the $j_s(H)$ peak. Above the minimum $S(H)$ shows a linear dependence, followed by a steep rise as the irreversibility field is approached. Two characteristic points determine the $S(H)$ behavior. The minimum value $S_{\text{min}} = (3\pm 1)\times 10^{-2}$ is very similar for all studied samples. It shows surprising independence on the temperature and oxygen content. The second characteristic point marks the transition to a much steeper $S(H)$ dependence, and corresponds to $S_t = 0.3\pm 0.1$, also

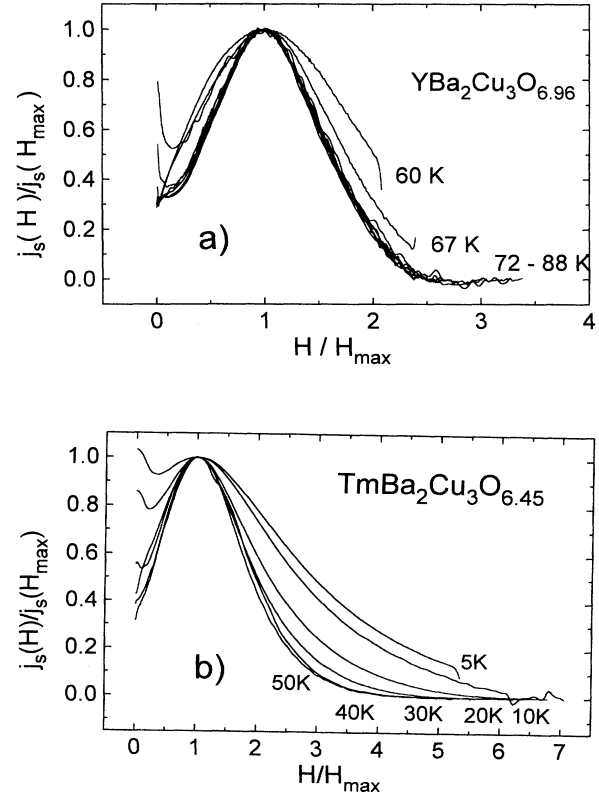


FIG. 2. The scaling behavior of the shielding currents for (a) low-oxygen-deficient $\text{YBa}_2\text{Cu}_3\text{O}_{6.96}$ (WU4) and (b) high-oxygen-deficient $\text{TmBa}_2\text{Cu}_3\text{O}_{6.45}$ (Z5) single crystals.

independent of the temperature and oxygen content. The magnetic field position of this point is close to the irreversibility line and similarly shifts to higher H with decrease of T and δ .

The characteristic feature of the fishtail behavior is a monotonic increase of H_{\max} with decreasing T . Such behavior is observed in the most part of the δ range (Fig. 5). However, for small δ a distinct nonmonotonic behavior appears in the intermediate-temperature range for most of the samples with $\delta < 0.1$. Moreover, in the

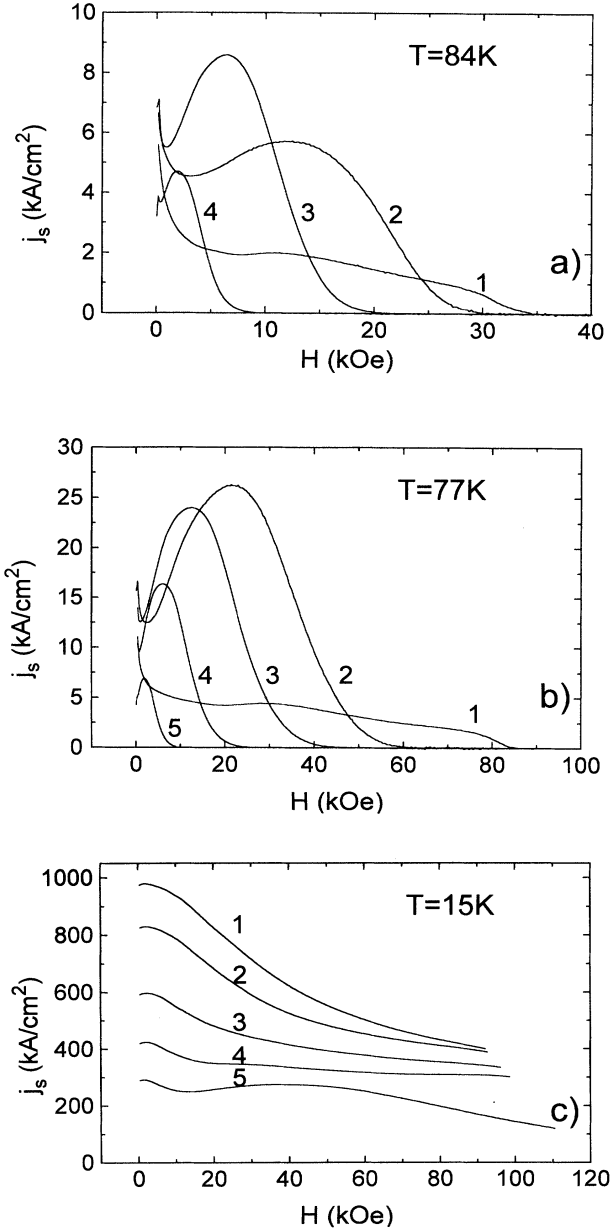


FIG. 3. The magnetic-field dependences of the shielding currents j_s for the YBa₂Cu₃O_y single crystal (WU3) at different temperatures T : (a) 84 K, (b) 77 K, (c) 15 K, for difference oxygen content: 1, 6.97; 2, 6.94; 3, 6.91; 4, 6.86; 5, 6.78 \pm 0.05. The annealing was made in sequence 2-1-3-4-5. The used sweep rate of the magnetic field 120 Oe/s corresponds to $E \sim 10^{-7}$ V/cm.

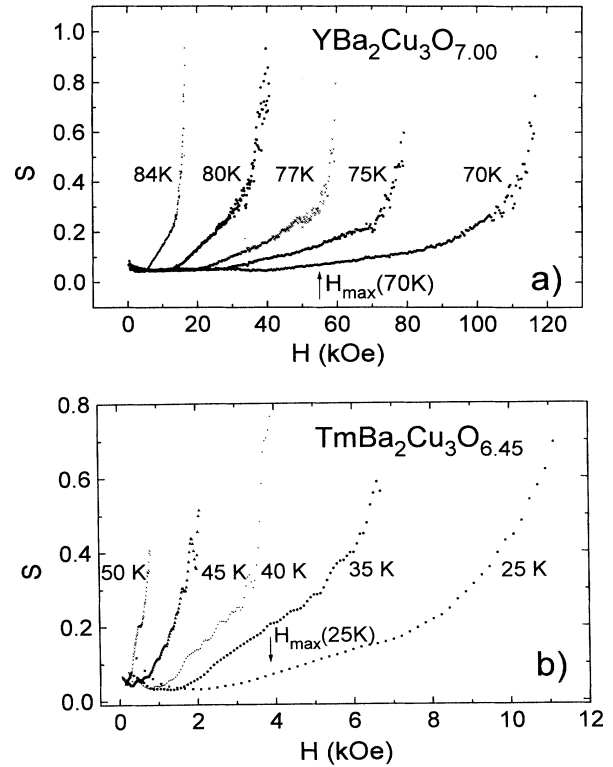


FIG. 4. The magnetic-field dependences of the normalized relaxation rate in the region of conventional fishtail behavior for (a) fully oxidized YBa₂Cu₃O_y (WU2, $y = 7.00 \pm 0.02$) and (b) high-oxygen-deficient TmBa₂Cu₃O_y (Z5, $y = 6.45 \pm 0.05$) single crystals. The arrow shows the position of the peak of the current H_{\max} for the temperature (a) 70 K and (b) 25 K.

region of decreasing H_{\max} the shape of the magnetization curve changes noticeably and corresponds to the second type of $m(H)$ behavior (Fig. 6). The ratio between H_{irr} and H_{\max} increases significantly, the maximum of $j(H)$ flattens transforming into a plateau, and then with further decrease of temperature into a double-peak structure. In the low-field region, the increasing behavior of

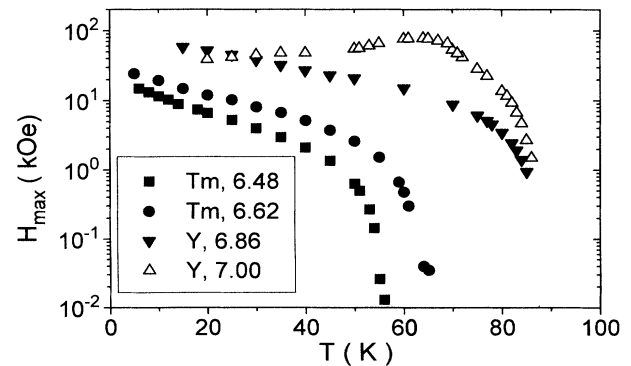


FIG. 5. The temperature dependences of the position of maximum H_{\max} in the $j(H)$ dependence for RBa₂Cu₃O_y single crystals (Z4, Z2, WU4, WU2) with different oxygen stoichiometry.

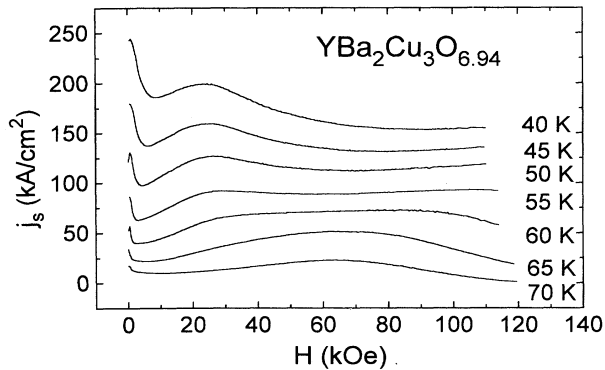


FIG. 6. The magnetic-field dependences of hysteresis width for different temperatures in the region of double-peak structure for $\text{YBa}_2\text{Cu}_3\text{O}_y$ (TWH, $y = 6.94 \pm 0.05$) single crystal.

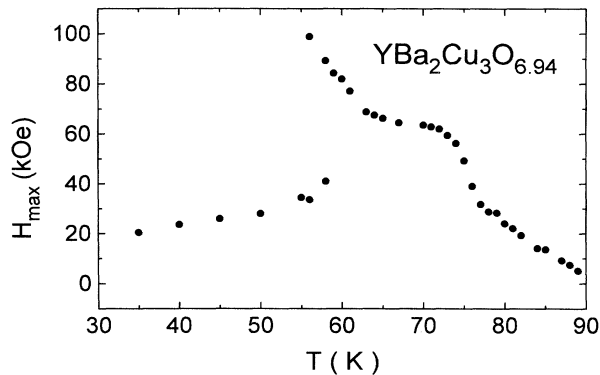


FIG. 7. The temperature dependence of the position of the maximum in $j(H)$ dependence for the $\text{YBa}_2\text{Cu}_3\text{O}_y$ (TWH, $y = 6.94 \pm 0.05$) single crystal with well-pronounced double-peak structure.

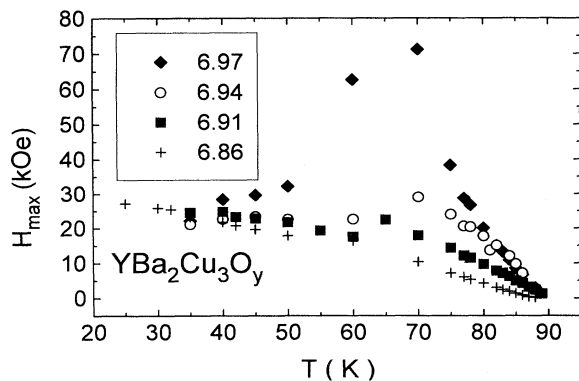


FIG. 8. The temperature dependences of the position of the maximum in $j(B)$ dependence for the $\text{YBa}_2\text{Cu}_3\text{O}_y$ single crystal (WU3) for different oxygen stoichiometries.

$\Delta m(H)$ is still conserved. However, the position of the low-field peak (or beginning of the plateau) shifts to *lower* H and saturates with decreasing temperature, in contrast to the usual fishtail behavior. On the contrary, the high-field maximum (or the end of the plateau) shifts to higher H similarly to the fishtail peak. The arising $H_{\text{max}}(T)$ dependence shows a drastic change in the region of the transition between the two types of $m(H)$ behavior (Fig. 7).

The low-field peak and high-temperature fishtail

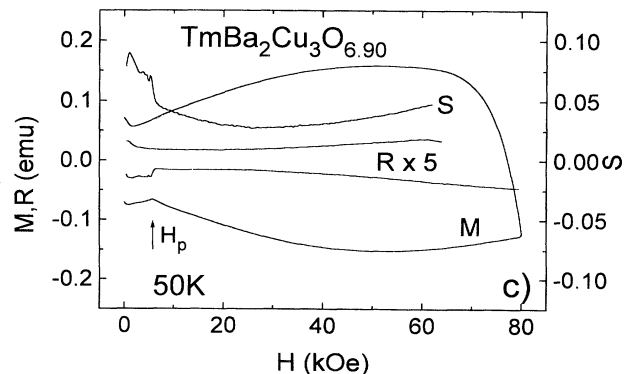
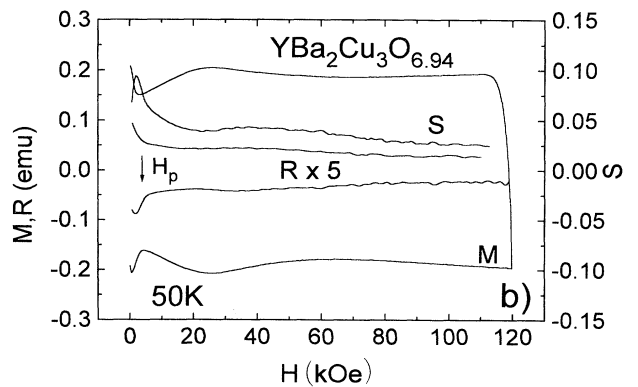
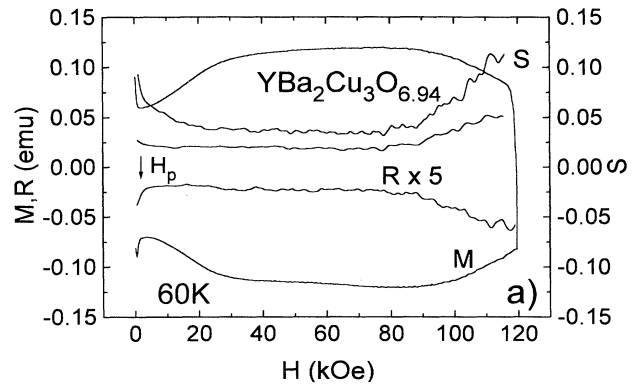


FIG. 9. The magnetic-field dependences of the magnetization, absolute R and normalized S relaxation rates for the $\text{YBa}_2\text{Cu}_3\text{O}_y$ (TWH, $y = 6.94 \pm 0.05$) single crystal, in the regions of (a) plateau ($T = 60$ K) and (b) double-peak $T = 50$ K structures and (c) for $\text{TmBa}_2\text{Cu}_3\text{O}_y$ (Z3, $y = 6.90 \pm 0.05$) single crystal showing no double-peak behavior. The arrow shows the field of full penetration H_p .

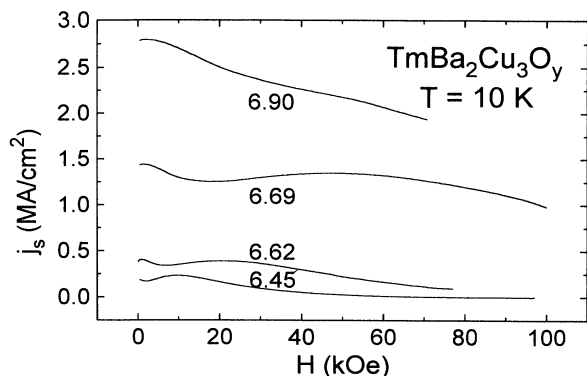


FIG. 10. The magnetic-field dependences of the shielding current at $T=10$ K for $\text{TmBa}_2\text{Cu}_3\text{O}_y$ single crystals (Z5, Z2, Z6, Z3) with different oxygen stoichiometries.

feature were found to have quite different properties. As was mentioned before, the field position of the fishtail peak was found to decrease fast with the increase of oxygen deficiency δ and temperature T . Figure 8 shows the temperature dependences $H_{\max}(T)$ for $\text{YBa}_2\text{Cu}_3\text{O}_{7-\delta}$ single-crystal WU3 with several different oxygen deficiencies δ . For the temperatures above the maximum of $H_{\max}(T)$, data represent the fishtail peak. At lower temperatures H_{\max} corresponds to the position of low-field peak in the double-peak structure. The high-field maximum was not observed for the studied temperature points. The low- H peak shows a very weak T and δ dependences which practically vanish at low temperatures (Fig. 8). Increased oxygen deficiency leads to the suppression of the $H_{\max}(T)$ anomaly, and above $\delta \sim 0.1$ only monotonic fishtail behavior is seen.

In the case of the double-peak structure, in correspondence with $m(H)$ behavior, the relaxation rate shows two minimum. It is worth mentioning that $S(H)$ for the low-field peak can show the minimum [Figs. 9(a) and 9(b)], being nearly “mirror” image of the $m(H)$ curve.⁴ However, the absolute relaxation rate $R = dM/dt(\ln \dot{H})$ is practically constant, so that $S(H)$ just reflects the behavior of

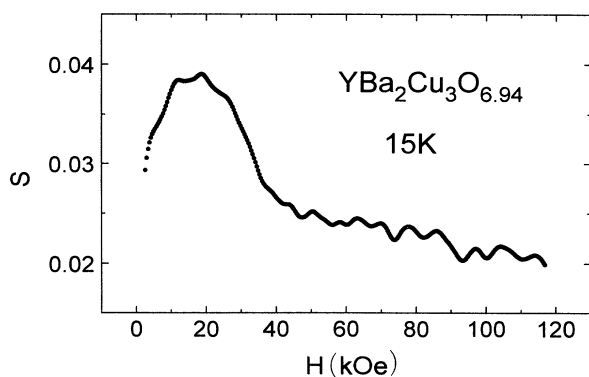


FIG. 11. The temperature dependences of normalized relaxation rate S obtained for increasing magnetic field in the low-temperature region for $\text{YBa}_2\text{Cu}_3\text{O}_y$ (TWH, $y=6.94 \pm 0.05$) single crystal.

$m(H)$. In the region of conventional fishtail behavior the minimum of S was observed to be always below $m(H)$ peak^{21,24} and no “mirror” image correspondence was found.

It is worth mentioning that, for intermediate T interval, in the region of the self-field it was observed a very sharp drop of the relaxation rate by nearly two times for the increasing branch of the magnetic field [Fig. 9(c)]. This anomaly was broadened for the most of the samples [Figs. 9(a) and 9(b)]. The position of this jump is very close to the field of the full penetration H_p . It is followed by the sharp kink in the field dependence of the magnetization and by the jump in the differential susceptibility dm/dH .²¹

It is necessary to stress that double-peak or plateau structure at intermediate temperatures was not a general feature for all of studied samples. Some of them showed a transition from the fishtail behavior directly to monotonic $m(H)$ decrease at low temperatures. A correlation with sample preparation procedure was not found for the samples grown in the same batch, both types of the behavior can be observed.

For the lowest temperatures ($T < 20$ K for $\delta=0$) the third type of $m(H)$ behavior with only a monotonic decrease of the current is found in the case of small oxygen deficiency. With the decrease of oxygen content this temperature region becomes rapidly narrower and disappears. For $\delta > 0.3$ the fishtail effect was observed down to the lowest measured temperature 4.2 K (Fig. 10). This third type of $m(H)$ behavior is characterized by small nearly constant S values close to $(2-3) \times 10^{-2}$ at high fields, and by a broad hump in the region of the penetration field (Fig. 11).

DISCUSSION

In our analysis of the experimental results we shall consider, first, the possible reasons of the fishtail anomaly and discuss the observed universal behavior of the relaxation rates. After this we shall discuss the other two types of magnetization curves found in $\text{RBa}_2\text{Cu}_3\text{O}_y$ single crystals.

For the explanation of the peak of the current vs field (peak effect) several mechanisms were proposed. They may be divided into two classes. In the first case, the increase of the current is caused by enhancement of the elementary pinning force f_i for one vortex on one center. This effect is ordinary connected with the precipitates of a second phase which for increasing magnetic field become normal conducting,¹ or have growing interaction energy with vortices due to increasing difference of intrinsic parameters.^{2,3,5} Recently a model has been proposed relating the increase of f_i to the proximity effect of normal inclusions.²⁵ The decrease of the current at high magnetic field is then related to granularity produced by the intersection of normal¹ or reversible impurity regions⁵ or with exceeding the H_{c2} or H_{irr} of the second phase.^{1,3,5}

The significance of granularity was rejected by transport²⁶ and by magnetic length scale measurements.^{3,27} Furthermore the results obtained here make a connection

of the peak with precipitates of a second phase very doubtful. Because it would require a phase with T_c only 2–4 K lower than the matrix, and critical parameters that changed synchronically with those of the matrix for different oxygen contents. First property is needed to raise the fishtail just below T_c , whereas the second provides the observed scaling of H_{\max} and H_{irr} . Such a specific second phase looks highly improbable, and microstructural analysis has not confirmed existence of any suitable second phase.

The second group of explanations connects the peak effect with the interplay between pinning and intervortex interactions. In one of the first models Pippard⁶ explained the increase of the current with magnetic field by the effect of the spatial synchronization (adjustment) of the vortex lattice with pinning centers. If one or more of the elastic constants becomes small, then vortex-vortex interaction decreases compared with the pinning interaction and this may produce a favorable condition for synchronization.

For any array of periodic pinning centers, the synchronization is not dependent on elastic properties, and occurs when the concentration of vortices is equal to the density of pinning centers. This situation is related to the matching mechanism⁸ characterized by a temperature-independent peak position. However, when the distribution of the distances between pinning centers is very broad, or when their concentration is very high, we have to deal with the situation in which the adjustment of vortices is reached for fields significantly below the matching field. The calculation of the resulting critical current for such a disordered case is highly dependent on the model used for the solution of the summation problem of vortex-vortex and vortex-pinning interaction. This problem is closely related to the degree of vortex lattice deformations. In the case of weak pinning, the pinned lattice is usually described using only elastic deformations.¹⁰ Several models emphasize the role of plastic deformations produced by the shearing of the vortices around pinning centers.^{28–32} One can expect plastic deformations to become increasingly important approaching the melting point of the vortex lattice due to the softening of C_{66} .

In elastic collective pinning theory,¹⁰ the increase of the current is connected with the transition to the nonlocal limit when the tilt modulus C_{44} sharply decreases. In this case the size of the elastically deformed correlated region (small bundles) decreases, thus increasing the pinning force per unit volume produced by the fluctuations inside this correlated volume. The decrease of the transverse bundle size is limited by the intervortex distance a_0 . In this case we have to deal with the single vortex pinning when the pinning force reaches its largest value due to the maximal adjustment of the vortex to the fluctuating pinning centers. Generally speaking, in this model the increase of $j(H)$ is connected with decreased order in vortex lattice, which is produced by the transition from the large bundles having extensive correlated regions to the amorphous state of the single vortices. The concentration of the vortices is however significantly below matching value. The further decrease of the current above the peak in this model is connected with the field

dependence of intrinsic parameters approaching H_{c2} .

Another reason which may limit the increase of the current growth may arise from the shear-stress limitation of the current in a vortex lattice as proposed by Kramer.^{7,28} Using the Kramer approach for the description of plastic deformations, Wördenweber²⁹ succeeded in reaching a quantitative agreement with experiment on epitaxial YBCO films. Furthermore, for easy flux shear it was pointed out the importance of weak channels originating from the morphology of the sample, e.g., grain boundaries.³⁰ Another approach considering shear produced by avalanche flux flow was proposed in Ref. 31. These approaches result in different exact expressions for the shear limited current. However, they may be reduced to the relation

$$j_s \sim \frac{C_{66}}{BW}, \quad (1)$$

where W is the characteristic length determined by the width of shearing vortex channels. In numerical simulations the existence of such channels was confirmed.³² The importance of plastic deformations for $\text{YBa}_2\text{Cu}_3\text{O}_{7-\delta}$ in the high-temperature region follows from the analysis of the flux profile measurements.³³

The model developed by Jensen, Brechet, and Brass³⁴ for plastic flow predicts, for the case of weak pinning, the transition from coherently moving vortex lattice with $W \rightarrow \infty$ to broad channels with $W \gg a_0$, and finally to narrow channels $W = a_0$ with the increase of magnetic field. Their expression for the current is also consistent with the Eq. (1).

For the shear modulus determined by

$$C_{66} = \frac{\Phi_0 B (1-b)^2}{(8\pi\lambda)^2}, \quad (2)$$

valid for $b = B/B_{c2} < 0.3$ and regular vortex lattice,³⁵ Eq. (1) gives a critical current increasing with magnetic field in the case of decreasing channel width W . Consequently in this approach the increased disorder in the vortex lattice leads also to the increase of the current.

Wördenweber and Kes¹¹ explained the peak effect seen in an amorphous Nb_3Ge thick film by a transition from the ordered lattice to the amorphous state with the simultaneous two-dimensional–three-dimensional (2D–3D) crossover. Recently a model describing the peak effect in the flux flow regime was proposed by Koshelev and Vinokur;³⁶ it is connected to the transition from a coherently moving vortex lattice to the amorphous state, as the melting point is approached.

Summarizing, we may conclude that several of the existing models of peak effect are based on the idea of increased disorder in the vortex system providing better synchronization of the vortices with pinning centers, determined by the interplay between vortex-vortex and vortex-pinning interaction. Such behavior is expected in the region of intermediate pinning strength. The pinning must be strong enough to provide irreversibility, but the correlation radius must significantly exceed intervortex distance. The fishtail feature disappears for the case of strong pinning in YBCO epitaxial films and melt-textured

samples. However, in more perfect melt-texture without the (211) phase, a fishtail maximum does indeed appear (Fig. 12).

We believe that such a general approach is valid both for the case of the peak effect in conventional superconductors and for the fishtail feature in a HTSC. In the first case, the melting point B_m is close to B_{c2} . However in a HTSC, large κ , and especially large anisotropy $\alpha^2 = M_c / M_{ab}$ lead to^{37,38}

$$B_m(T) \approx \beta_m \frac{c_L^4}{Gi} B_{c2}(0) \left[1 - \frac{T}{T_c} \right]^2 \quad (3)$$

being significantly below B_{c2} , where

$$\beta_m \approx 5 ,$$

$$c_L \sim 0.1 - 0.2 ,$$

$$Gi = 16\pi^3 \kappa^4 \alpha^2 (k_B T_c)^2 / \Phi_0^3 H_{c2}(0) .$$

For the disordered superconductors, the second kind of melting transition is expected with gradual vanishing of C_{66} at B_m , whereas Eq. (2) remains valid far below transition. For the model of a shear limited current, the dome-like shape of $j_s(H)$ reflects the behavior of C_{66} . The observed scaling of $j(H)$ and $S(H)$ may be then connected with a universal variation of C_{66} as the melting transition is approached. In such an approach we can still expect differences in the shape of the $j(H)$ peak for the conventional superconductors and HTSC's, particularly due to the different behavior of C_{66} and of the elementary pinning force in the region approaching B_m and the more important role of fluctuations in the HTSC.

At the present time it is not possible to make a direct comparison of the existing theories with experiment. The main reason for this is that all existing theories are based on expression (2) for C_{66} which is strictly valid only for zero temperature and a regular lattice. This approach provides vanishing of C_{66} only at B_{c2} . The realistic expression providing $C_{66} \rightarrow 0$ at the melting point is still not derived. Another reason is that most of these theories do not consider the flux creep regime, and so do not give a realistic description of the experiment.

An important question is what kind of pinning centers

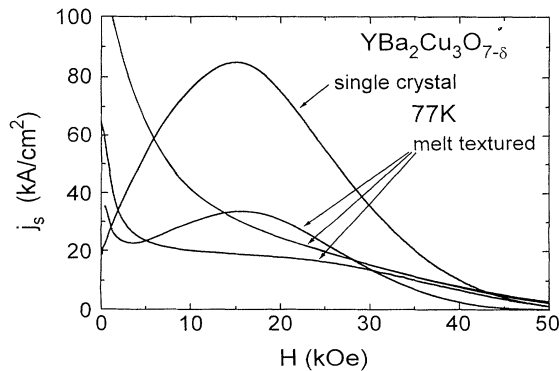


FIG. 12. The magnetic-field dependences of the shielding currents for $T=77$ K in $\text{YBa}_2\text{Cu}_3\text{O}_x$, single crystal (1) and different melt-textured samples.

are involved in fishtail behavior. The results obtained for the samples of low oxygen deficiency point to oxygen vacancies being important for the peak of the current arisen at high temperatures. The strength of pinning is determined mainly by two factors: (i) by the strength of the oxygen disorder and (ii) by the values of intrinsic parameters λ and ξ . For the case of large δ values the oxygen disorder does not change significantly with δ , and the behavior of current is governed by the change of intrinsic parameters as discussed before.³⁹ However for the case of small δ , the values of λ and ξ decrease more slowly, and the suppression of oxygen disorder becomes a dominant factor leading to the decrease of the measured currents (Fig. 3). Simultaneously, a sharp increase of the irreversibility line with lower δ in contrast to the decreasing current points to the melting nature of the transition at B_{irr} . In the case of depinning we should expect j_s and B_{irr} to both increase or to both decrease.

Next we consider the flux creep behavior observed. For the analysis of relaxation rates we shall use the quite general expression for thermally activated flux creep⁴⁰

$$E = E_c \exp \left[- \frac{U(B, T, j)}{kT} \right] \quad (4)$$

which describes the current-voltage characteristic of the superconductor. The characteristic voltage E_c , which determines the crossover to activationless vortex movement, is dependent on the parameters of jumping vortex bundles and may be roughly estimated from the Bardeen-Stephen⁴¹ relation

$$E_c \sim \frac{\rho_n B}{B_{c2}} j_c$$

which gives $E_c \sim 1$ V/cm for the typical parameters $\rho_n \sim 10^{-4}$ Ω cm, $B/B_{c2} \sim 10^{-2}$, $j_c \sim 10^6$ A/cm². The conventional magnetic measurement procedure with a constant sweep rate of the magnetic field (providing $E = \text{const}$ above the self-field region) corresponds to the expression

$$U(B, T, j)/kT = \ln \frac{E_c}{E} , \quad (5)$$

which is only weakly dependent on temperature and magnetic field. According to Refs. 42 and 43 the normalized relaxation rate is determined by the slope of $\log E$ - $\log j$ curve

$$S = \frac{d \ln j}{d \ln E} = \frac{kT}{j [\partial U(B, T, j) / \partial j]} = - \frac{1}{\ln(E_c/E)} \frac{d \ln j}{d \ln U(B, T, j)} . \quad (6)$$

Equations (5) and (6) determine the measured relaxation rate, which generally does not reflect the behavior $\partial U(B, T, j) / \partial j$ for $j = \text{const}$. Considering the characteristic behavior for a collective creep or vortex-glass relation^{38,44}

$$U(B, T, j) = U_0(B, T) \left(\frac{j_0}{j} \right)^\mu \quad (7)$$

it is possible to obtain nearly a temperature- and magnetic-field-independent normalized relaxation rate:

$$S = \frac{1}{\mu \ln(E_c/E)}. \quad (8)$$

For the regime of small bundles^{38,44} with $\mu = \frac{3}{2}$ in the experimental range $E \sim (10^9 - 10^{-8})$ V/cm, using typical $E_c \sim 1$ V/cm, the relaxation rate may be estimated as

$$S \approx 3 \times 10^{-2}.$$

This value is in good agreement with the relaxation rates observed in the region of the minimum of $S(H)$ dependence and at low temperature. In spite of the limited application of Eq. (7) for the description of the experimental E - j curves⁴⁵ we think the universal temperature and oxygen-independent $S = (2-4) \times 10^{-2}$ in the region of its minimum is determined by the discussed or a similar mechanism based on elastic deformations of the vortex lattice. The large increase of relaxation rate at low and high fields we tentatively attribute to the influence of plastic deformations arising in the region of melting and reentrant melting transitions.⁴⁶ The last transition could explain the anomalous jump in the relaxation rate and the kink in $m(H)$ dependence at low fields.

The second universal point in $S(H)$ dependence $S_i \approx 0.3$ observed near the irreversibility line can be connected with the melting transition.²⁴ This value in the approximation of powerlike $E \sim j^n$ curves corresponds to $n \approx 3$. Just this value is predicted for 2D Kosterlitz-Thouless melting transition.⁴⁷ For a 3D vortex-glass-vortex-liquid transition the theory⁴⁶ also predicts powerlike behavior. The experimental n values scatter from ~ 5 (Ref. 48) to ~ 2 .⁴⁹ This agrees with our observation of $S = 1/n = (0.2-0.4)$.

Next we discuss the dynamic explanation of the fishtail. In this model, based on the collective pinning mechanism, the increase of the current is related to a slower relaxation at higher magnetic field. The authors⁴ stated that the $S(H)$ dependence is a mirror image of the $j(H)$ curve. We observed the mirror behavior only at intermediate temperatures where the absolute relaxation rate is about constant. As we shall show later, this temperature interval is dominated by the matching of vortex and twin structures. In the region of the fishtail behavior no mirrorlike correspondence was found.^{21,24,45,50} Furthermore, this hypothesis is not supported by the observation that samples with and without the fishtail show qualitatively the same $S(H)$ behavior.⁴⁵ This approach does not describe the scaling behavior observed. Moreover, the relaxation explanation, based on no fishtail behavior for the critical current j_c , contradicts the prediction of increased critical current in the Larkin-Ovchinnikov model.¹⁰

It is necessary to mention that the collective creep theory based on expression (2) for C_{66} leads to the current increasing with the magnetic field both for the regime of small and large bundles. Considering the case $j \ll j_c$ we shall use the equation

$$j = j_\mu \left[\frac{kT}{U_\mu} \ln \frac{E}{E_\mu} \right]^{1/\mu}. \quad (9)$$

This relation follows from Eqs. (4) and (7) and corresponds to Eqs. (4.69) of Ref. 38 with replacement of t by E . Here E_μ is a crossover voltage corresponding to characteristic time t_0 . In principle t_0 and E_μ must also be dependent on B . We shall neglect this logarithmic dependence in our analysis.

The collective creep theory predicts the sequence of transitions (from the single vortex to the small bundle and next to the large bundle creep) with increase of the magnetic field and decrease of the current. References 38 and 44 give expressions for j_μ and U_μ :

$$\begin{aligned} j_{sb} &\approx j_{sv} \left[\frac{L_c}{a_0} \right]^{7/5}, & U_{sb} &\approx U_{sv} \left[\frac{a_0}{L_c} \right]^{1/5}, \\ j_{lb} &\approx j_{sb} \left[\frac{a_0}{\lambda} \right]^2, & U_{lb} &\approx U_{sb} \left[\frac{\lambda}{a_0} \right]^3. \end{aligned} \quad (10)$$

The theory predicts magnetic-field-independent parameters in the single-vortex state (j_{sv}, U_{sv}) and $L_c \approx \xi(j_0/j_{sv})^{1/2}$ where j_0 is the depairing current. In the case of the single-vortex creep, this leads to the absence of B dependence for $j(B)$. On the other hand, increasing $j(B) \sim B^{19/30}$ and $\sim B^{1.5}$ may be obtained for small and large bundles, respectively. There then appears the problem of explaining the observed $j(H)$ decrease. This could be connected with the approach of j_c , where Eq. (9) becomes inapplicable.⁵¹ However, this contradicts the downward shift of peak position observed with decrease of voltage E (Ref. 26) or increase of time for relaxation.⁵ We should expect the opposite behavior, because Eq. (9) must become valid with the decrease of the current. This also disagrees with the transport²⁶ and long-time relaxation measurements⁴⁵ when it is possible to consider in the decreasing branch $j(H)$ changes of the current exceeding 1 order of magnitude. The slope $d(\ln E)/d(\ln j)$ at high currents still significantly exceeds 1, which expected approaching the flux flow regime. Then low currents should satisfy the relation $j \ll j_c$, which contradicts to the given above explanation for $j(H)$ decrease.

However, it is worth mentioning that dynamic effects connected with the dependence of activation energy on the current and magnetic field may be important as can be seen from Eq. (5). For a mechanism which provides an increase of activation energy for decreasing current and increasing magnetic field or vice versa, the increase of the magnetic field induces a growth of the current to provide constant U/kT .⁵² Such dynamic effects produced by the flux creep can be present independently of j_c showing or not showing peak effect.

Next we analyze the intermediate-temperature range. The weak dependence of low-field $j_s(H)$ peak position on temperature and oxygen content points to a different origin from that discussed above for the fishtail effect. We think that this peak has a matching origin produced by extended strong defects. In $\text{Bi}_2\text{SrCa}_2\text{CuO}_y$ single crystals the temperature-independent peak of the current at $H_{\max} \sim 1$ kOe was related to the matching produced by the net of dislocations found in these samples.⁵³ The value of the maximum field 2–5 T points to the twin structure in the $\text{RBa}_2\text{Cu}_3\text{O}_y$ sample. The characteristic

smallest size of twins given by a number of papers (e.g., Ref. 54) is in the range $d \sim 10\text{--}50$ nm. This is in agreement with the expected matching field $H_m \approx \Phi_0/d^2$. Such a conclusion is further confirmed that this peak was not observed in the untwinned $\text{TmBa}_2\text{Cu}_3\text{O}_{7-\delta}$ single crystal.³ However we have found that some of the crystals without this second type of $m(H)$ behavior are twinned. This could be explained by the significantly different size of twins in those samples shifting the matching peak in the self-field region or above the maximum available field of 12 T.

Recently we obtained the direct confirmation for the connection of intermediate-temperature $m(H)$ structure with twins using stress-induced detwinning.⁵⁵ The detwinned single crystal showed conventional fishtail behavior in the temperature interval where this double peak was observed in the twinned state. The last feature totally disappeared and the detwinned sample showed a direct transition from fishtail to monotonic low-temperature behavior. The position of the fishtail peak was between the initial two peaks. This points to the interference of two mechanisms producing the fishtail and matching peak. Such interference can be the reason for the weak $j(H)$ dependence between two peaks, which contrasts with the large $j(H)$ variations at low temperatures [Figs. 3(c) and 6, 9, and 10]. The disappearance of this structure with the decrease of oxygen content may be related to the shift of the fishtail peak below the matching field. According to our previous analysis of the fishtail nature we can expect a disordered vortex state above the maximum of the current. In this situation the peak produced by matching of the vortex lattice with the defect structure should disappear.

The behavior of $j_s(H)$ at low temperatures might be connected with the single-vortex pinning. However, the apparent $j_s(H)$ dependence is in contradiction with such a hypothesis. For estimation of the crossover field the expression from Ref. 38 may be used:

$$B_{sb} = \beta_{sb} \frac{j_c}{j_0} H_{c2}, \quad (11)$$

with $\beta_{sb} \approx 5$. Using $H_{c2} = 10^2$ T and $j_0 = 3 \times 10^8$ A/cm² for $j_c = 10^6$ A/cm² at low temperatures it is possible to find $B_{sb} \sim 2$ T. This field corresponds to comparable values of vortex-vortex and vortex-defect interaction. Consequently, the applicability of the field-independent single-vortex expressions^{44,49} is limited by $B \ll B_{sb} \sim 2$ T. The studied field range up to 12 T may correspond mostly to the pinning of the small bundles. This is consistent with the observed field-independent S value in this region. For low fields single-vortex pinning may be important. This agrees with the increase of S at small fields which we can expect for single-vortex pinning with $\mu = \frac{1}{7}$ according to Eq. (8). However, the analysis of this region is complicated by the large self-field comparable with B_{sb} . The absence of an increasing current in the region of small bundles for low temperatures can be connected with values of j_s approaching J_c , where Eq. (9) becomes invalid. Another possibility may be the slipping of vortices along the twin planes.^{55,56} This mechanism may occur at low T when the pinning strength along the twin

boundary falls below bulk pinning. In accordance with this, detwinning spreads the fishtail behavior to the low T interval too.⁵⁵

The question of what are the pinning centers at this region cannot be clarified yet. The data presented in Fig. 3 point against the oxygen vacancies being dominant at low temperatures.

CONCLUSIONS

In this work we present a study of the influence of oxygen content on the magnetization and relaxation of $R\text{Ba}_2\text{Cu}_3\text{O}_{7-\delta}$ ($R = \text{Y, Tm}$) single crystals for $0 \leq \delta \leq 0.55$. For the highly oxygenated samples, three different types of $m(H)$ and $S(H)$ behavior may be distinguished. The high-temperature region corresponds to the ordinary fishtail. In this case the peak position H_{max} shifts to higher H with temperature decrease, and correlates with H_{irr} . Sample-dependent scaling was observed for the $j(H)$ dependences. The normalized relaxation rate shows a minimum at a field close to one-half of that at the position of the $j_s(H)$ peak, and a sharp increase near the irreversibility line. The characteristic S_{min} and S_t values show a surprising independence of temperature and oxygen content. The samples with low oxygen deficiency showed a decrease of the current with a simultaneous increasing B_{irr} . This points to the importance of oxygen disorder for the pinning, and stresses the melting nature of the irreversibility line. We connect the observed increase of the current to synchronization effects of the increased disorder in the vortex lattice. The universal vanishing of C_{66} at the melting transition probably underlies the observed $M(H)$ scaling behavior.

In the intermediate-temperature region a double-peak structure is observed. The low-field peak position showed a weak temperature and δ dependence. Its origin is related to the matching effect between the vortex lattice and the twin structure in the sample. The relaxation rate in this region also acquires a second minimum. With $\delta > 0.1$, the second peak disappears when the fishtail position shifts below the matching field.

The low-temperature region is characterized by a monotonic decrease of $j(H)$ and a nearly constant $S(H)$. The possible connection of the low-temperature regime with the pinning of small bundles or with the slipping of vortices along the twin planes is considered. For large δ , this region shrinks and disappears for $\delta \geq 0.3$.

ACKNOWLEDGMENTS

The authors appreciate useful discussions with E. H. Brandt, H. J. Jensen, A. E. Koshelev, and V. M. Vinokur. We are grateful to I. L. Maximov and W. Jahn for a critical reading of the manuscript and important suggestions and A. Will for technical assistance. A.A.Z. acknowledges support of Royal Society during his visit to Imperial College. This work was supported by the Bundesministerium für Forschung und Technology under Grant No. 13N6177, by Russian Scientific Council on HTSC Project No. 93173, Russian Fund for Fundamental Researchers, Grant No. 93-02-14768, Engineering and Physical Sciences Research Council and by NATO Linkage Grant No. HT931241.

- ¹M. Daeumling, J. M. Seutjens, and D. C. Larbalestier, *Nature* (London) **346**, 332 (1990).
- ²V. V. Moshchalkov, A. A. Zhukov, I. V. Gladyshev, S. N. Gordeev, G. T. Karapetrov, V. D. Kusnetsov, V. V. Metlushko, V. A. Murashov, V. I. Voronkova, and V. K. Yanovskii, *J. Magn. Magn. Mater* **90&91**, 611 (1990); A. A. Zhukov, V. V. Moshchalkov, V. V. Metlushko, G. T. Karapetrov, V. I. Voronkova, V. K. Yanovskii, and V. D. Kusnetsov, *Physica C* **185-189**, 2431 (1991).
- ³A. A. Zhukov, H. K pfer, S. A. Klestov, V. I. Voronkova, and V. K. Yanovskii, *J. Alloys Comp.* **195**, 479 (1993).
- ⁴L. Krusin-Elbaum, L. Civale, V. M. Vinokur, and F. Holtzberg, *Phys. Rev. Lett.* **69**, 2280 (1992).
- ⁵L. Klein, E. R. Yacoby, Y. Yeshurun, A. Erb, C. M ller-Vogt, V. Breit, and H. W hl, *Phys. Rev. B* **49**, 4403 (1994).
- ⁶A. B. Pippard, *Philos. Mag.* **19**, 217 (1969).
- ⁷K. E. Osborne and E. J. Kramer, *Philos. Mag.* **29**, 685 (1974).
- ⁸J. Petermann, *Z. Metall.* **61**, 724 (1970).
- ⁹A. M. Campbell and J. E. Evetts, *Critical Currents in Superconductors* (Taylor & Francis, London, 1972).
- ¹⁰A. I. Larkin and Yu. N. Ovchinnikov, *J. Low Temp. Phys.* **34**, 409 (1979).
- ¹¹R. W rdenweber and P. Kes, *Phys. Rev. B* **34**, 494 (1986).
- ¹²A. A. Zhukov, G. Perkins, L. F. Cohen, H. K pfer, J. T. Tottoy, A. D. Caplin, S. A. Klestov, H. Claus, V. I. Voronkova, and H. W hl, *Physica C* **235-240**, 2837 (1994).
- ¹³E. M. Parks *et al.*, *J. Solid State Chem.* **79**, 53 (1989).
- ¹⁴M. Kogachi *et al.*, *Jpn. J. Appl. Phys.* **28**, L609 (1989).
- ¹⁵R. Hauff, V. Breit, H. Claus, D. Herrmann, A. Knerim, P. Schweiss, H. W hl, E. Erb, and G. M ller-Vogt, *Physica C* **235-240**, 1953 (1994).
- ¹⁶V. I. Voronkova *et al.*, *JETP Lett.* **52**, 224 (1990).
- ¹⁷A. Erb *et al.*, *J. Cryst. Growth* **132**, 389 (1993).
- ¹⁸A. A. Zhukov, H. K pfer, S. N. Gordeev, W. Jahn, T. Wolf, V. I. Voronkova, A. Erb, G. M ller-Vogt, H. W hl, H. J. Bornemann, K. Salama, and D. Lee, in *Proceedings of the 7th International Workshop on Critical Currents in Superconductors*, Alpbach, Austria, 1994, edited by H. W. Weber (World Scientific, Singapore, 1994), p. 229.
- ¹⁹A. A. Zhukov, H. K pfer, V. A. Rybachuk, L. A. Ponomarenko, V. A. Murashov, and A. Yu. Martynkin, *Physica C* **219**, 99 (1994).
- ²⁰L. Pust, *Supercond. Sci. Technol.* **3**, 598 (1990).
- ²¹A. A. Zhukov, L. F. Cohen, G. K. Perkins, A. D. Caplin, S. A. Klestov, V. I. Voronkova, A. Marshall, and S. Abell, *Physica B* **194-196**, 1921 (1994).
- ²²K. A. Delin and T. P. Orlando, *Phys. Rev. B* **46**, 11 092 (1992).
- ²³L. Civale, M. W. McElfresh, A. D. Marwhich, F. Holtzberg, and C. Field, *Phys. Rev. B* **43**, 1373 (1991); M. Oussena, P. A. J. de Groot, A. Marshall, and J. S. Abell, *Phys. Rev. B* **49**, 1484 (1994).
- ²⁴L. F. Cohen, A. A. Zhukov, G. K. Perkins, H. J. Jensen, S. A. Klestov, V. Voronkova, S. Abell, H. K pfer, T. Wolf, and A. D. Caplin, *Physica C* **230**, 1 (1994).
- ²⁵K. I. Kugel, T. Matsushita, E. Z. Meilikhov, and A. L. Rakhmanov, *Physica C* **228**, 373 (1994).
- ²⁶S. N. Gordeev, W. Jahn, A. A. Zhukov, H. K pfer, and T. Wolf, *Phys. Rev. B* **49**, 15 420 (1994).
- ²⁷L. F. Cohen, J. R. Laverti, G. K. Perkins, A. D. Caplin, and W. Assmus, *Cryogenics* **33**, 352 (1993).
- ²⁸E. J. Kramer, *J. Appl. Phys.* **44**, 1360 (1973).
- ²⁹R. W rdenweber and M. O. Abd-El-Hamed, *Supercond. Sci. Technol.* **5**, 379 (1992); R. W rdenweber, *Phys. Rev. B* **46**, 3076 (1992).
- ³⁰J. E. Evetts and C. J. G. Plummer, in *Proceedings of the International Symposium on Flux Pinning and Electron Properties in Superconductors*, edited by T. Matsushita, K. Yamafuji, and F. Irie (Matsukuma, Fukuoka, 1985), p. 146; D. Dew-Hughes, *IEEE Trans. Magn. MAG-23*, 1172 (1987); *Philos. Mag. B* **55**, 459 (1987).
- ³¹T. Matsushita and H. K pfer, *J. Appl. Phys.* **63**, 5048 (1988).
- ³²H. J. Jensen, A. Brass, and A. J. Berlinsky, *Phys. Rev. Lett.* **60**, 1676 (1988).
- ³³H. K pfer *et al.* (unpublished).
- ³⁴H. J. Jensen, Y. Brechet, and A. Brass, *J. Low Temp. Phys.* **74**, 293 (1989).
- ³⁵E. H. Brandt, *J. Low Temp. Phys.* **26**, 735 (1977).
- ³⁶A. Koshelev and V. Vinokur, *Phys. Rev. Lett.* **73**, 3580 (1994).
- ³⁷A. Houghton, R. A. Pelcovits, and A. Sudb , *Phys. Rev. B* **40**, 6763 (1989).
- ³⁸G. Blatter, M. V. Feigel'man, V. B. Geshkenbein, A. I. Larkin, and V. M. Vinokur, *Rev. Mod. Phys.* (unpublished).
- ³⁹J. G. Ossandon, J. R. Thompson, D. K. Christen, B. C. Sales, H. R. Kerchner, J. O. Thomson, Y. R. Sun, K. W. Lay, and J. E. Tkaczyk, *Phys. Rev. B* **45**, 12 534 (1992).
- ⁴⁰H. G. Schnack, R. Griessen, J. G. Lensink, and Wen Hau-Hu, *Phys. Rev. B* **48**, 13 178 (1993).
- ⁴¹J. Bardeen and M. J. Stephen, *Phys. Rev. A* **140**, 1197 (1965).
- ⁴²A. A. Zhukov, *Solid State Commun.* **81**, 983 (1992).
- ⁴³C. J. van der Beek, G. J. Nieuwenhuys, P. H. Kes, H. C. Schnack, and R. Griessen, *Physica C* **197**, 320 (1992).
- ⁴⁴M. V. Feigel'man, V. B. Geshkenbein, A. I. Larkin, and V. M. Vinokur, *Phys. Rev. Lett.* **63**, 2303 (1989).
- ⁴⁵H. K pfer, S. N. Gordeev, W. Jahn, R. Kresse, R. Meier-Hirmer, T. Wolf, A. A. Zhukov, K. Salama, and D. Lee, *Phys. Rev. B* **50**, 7016 (1994).
- ⁴⁶D. S. Fisher, M. P. A. Fisher, and D. A. Huse, *Phys. Rev. B* **43**, 130 (1991).
- ⁴⁷V. Ambegaokar, B. I. Halperin, D. R. Nelson, and E. D. Siggia, *Phys. Rev. B* **21**, 1806 (1990).
- ⁴⁸J. Deak, M. McElfresh, J. R. Clem, Z. Hao, M. Konczykowski, R. Muenchausen, S. Foltynand, and R. Dye, *Phys. Rev. B* **49**, 6270 (1994); Qiang Li, H. J. Wiesmann, M. Suenaga, L. Motowidlow, and P. Haldar, *ibid.* **50**, 4256 (1994).
- ⁴⁹R. H. Koch, V. Foglietti, W. J. Callagher, G. Koren, A. Gupta, and M. P. A. Fisher, *Phys. Rev. Lett.* **63**, 1511 (1989); T. K. Worthington, E. Olsson, C. S. Nichols, T. M. Shaw, and D. R. Clarke, *Phys. Rev. B* **43**, 10 538 (1991); N. C. Yeh, D. S. Reed, W. Jiang, U. Kriplani, C. C. Tsuci, C. C. Chi, and F. Holtzberg, *Phys. Rev. Lett.* **71**, 4043 (1993), and references therein.
- ⁵⁰M. Jirsa, A. J. J. van Dalen, M. R. Koblischka, G. Ravi Kumar, and R. Griessen (Ref. 18), p. 221.
- ⁵¹L. Civale, L. Krusin-Elbaum, J. R. Thomson, and F. Holtzberg, *Phys. Rev. B* **50**, 7188 (1994).
- ⁵²G. K. Perkins, L. F. Cohen, A. A. Zhukov, and A. D. Caplin, *Phys. Rev. B* **51**, 8513 (1995).
- ⁵³G. Yang, P. Shang, S. D. Sutton, I. P. Jones, J. S. Abell, and C. E. Gough, *Phys. Rev. B* **48**, 4054 (1993).
- ⁵⁴M. Rand, J. I. Langford, A. Drake, and J. S. Abell, *Cryogenics* **33**, 291 (1993); J. Chrosch and E. K. H. Salje, *Physica C* **225**, 111 (1994).
- ⁵⁵A. A. Zhukov, H. K pfer, M. Kl ser, H. Klaus, and H. W hl (unpublished).
- ⁵⁶M. Oussena, P. A. J. de Groot, S. J. Porter, R. Gagnon, and L. Taillefer, *Phys. Rev. B* **51**, 1389 (1995).